



Research Article

## Rice Acreage Estimation of Ludhiana District using Sentinel-1A Time Series Data

ANURADHA SHARMA, JOYDEEP MUKHERJEE\*, V.K. SEHGAL, D. CHAKRABORTY AND D.K. DAS

*Division of Agricultural Physics, ICAR-Indian Agricultural Research Institute, New Delhi-110012*

### ABSTRACT

Rice is a staple food for half of the world's population. In term of rice production India is in second position in the world where rice production plays a great contribution to the economy of the country. Thus there is a requirement of information on rice area to meet the population consumption needs in an effective manner. Conventional methods are generally adopted to collect the statistics of rice area, however these are time consuming, labor dependent and cost effective. Recent space borne remote sensing such as Synthetic Aperture Radar (SAR) is proven to be a competent tool in mapping and monitoring the rice fields on a regional scale. In this study, Sentinel-1A C-band time series data of kharif season 2018 has been taken into account for the mapping of rice fields in the Ludhiana district of Punjab which is well known for the cultivation of rice on a large scale. With the availability of dual polarization of Sentinel-1A, the temporal characteristics of backscattering coefficient values with the rice growth indicated that VH polarization is more sensitive to rice growth than the VV polarization. Threshold based classification approach has been used where thresholds were estimated to classify the rice and non-rice area of the region. The reference data such as Sentinel-2 and Google Earth imagery were utilized to collect the signatures of rice and non-rice such as built up and water features. The overall accuracy of classification obtained as 92.64% and kappa coefficient as 0.85. The total area estimated from classification is 2.54 lac ha which is quite close to reported as 2.57lac ha.

**Key words:** Synthetic Aperture Radar (SAR), Rice mapping, Sentinel-1A, Sentinel-2, Threshold, Classification

### Introduction

Rice is one of the essential staple food on which half of the world's population is dependent. Its cultivation comprises more than 12% of the global cropland distribution area (FAOSTAT). It requires significantly more water than any other food grains (Ishitsuka, 2018). Therefore it plays a substantial role not only in food security purpose but also in environmental related issues such as climate change, water usage as well as health

issues like disease transmission (Dong & Xiao, 2016). In India, its production is largely contributed to the national economy of the country. As India is the second largest producer of rice after China in the world with diverse rice cropping system hence it required to meet the need of rice consumption in the country through cultivation and importing practices. However, due to scarcity of water resource by increasing demand of human consumption, industrial use and power generation have caused serious concerns to environment (Holecz *et al.*, 2000). These leads to the requirement of an effective monitoring of

\*Corresponding author,  
Email: [joydeep.icar@gmail.com](mailto:joydeep.icar@gmail.com)

paddy fields for food security and agricultural mitigation point of view in order to identify and forecast rice production (Park *et al.*, 2018).

Available conventional methods for monitoring rice areas are ground based sample surveys which are expensive, labor intensive, manual and time consuming. Space-borne remote sensing methods offers an alternative as well as effective approach for mapping and monitoring paddy fields at regional to global scale (Dong & Xiao, 2016; Park *et al.*, 2018). In optical remote sensing, sensors like MODIS and AVHRR datasets with high temporal resolution and coarser spatial resolution were employed in the visible and IR region for the rice classification using spectral bands and indices namely Normalized Difference Vegetation Index (NDVI), Enhanced Vegetation Index (EVI), Land Surface Water Index (LSWI) (Teluguntla *et al.*, 2015), Normalized Difference Flooding Index (NDFI) while finer spatial resolution satellites viz. LANDSAT MSS/TM/OLI (Genc *et al.*, 2014; McCloy *et al.*, 1987; Okamoto and Fukuhara, 1996; Zhang *et al.*, 2018) and SPOT (Turner and Congalton, 1998) have also been explored for examining the phenological growth stage of rice. Several approaches discussed for paddy mapping using reflectance is given in a detailed review by (Dong and Xiao, 2016). On contrary, these sensors have limitations which restricts them

during rice transplantation in monsoon season that contains thick cloud cover. In such condition active microwave remote sensing provides a valuable tool for mapping as well as monitoring the growth of the rice.

Synthetic Aperture Radar (SAR) has the potential of being not affected by cloud and atmospheric conditions (Stroppiana *et al.*, 2019) and provide vital information even during rice transplanting period of time. The interaction of SAR with rice growth stage are demonstrated by (Clauss *et al.*, 2017) in Figure 1. The early stage of rice which is flooded acts as a smooth surface and causes specular reflection. After the rice transplant, very little backscattering takes place. As the rice plant grows, double and multiple scattering causes the increase in backscattering. There is continuous increase in backscattering till the heading stage. In later ripening stage, the volume scattering become dominant and backscatter decreases. Thus SAR distinguish well-developed rice from the water surface and other crop in an efficient manner (Bouvet *et al.*, 2009).

Kurosu *et al.* (1995) were the first who attempted rice mapping using ERS -1 C band SAR data. Later several studies discussed the competence of SAR data in C, X, and L using ERS-1 (Toan *et al.*, 1997), RADARSAT & RADARSAT 2 (Hoang *et al.*, 2016; Ribbles *et*

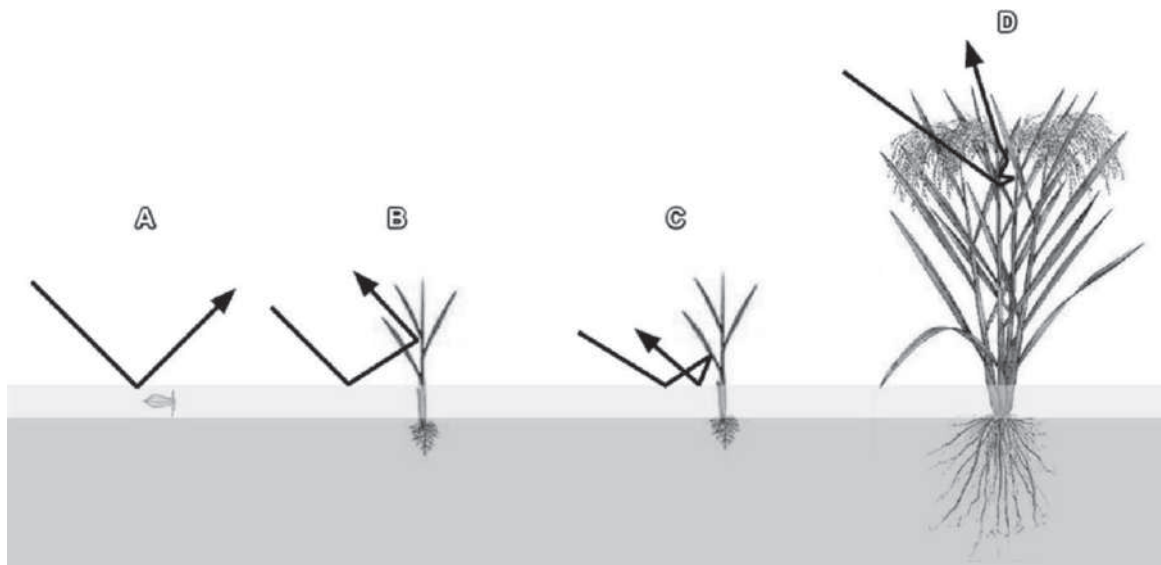


**Fig. 1.** Interaction of backscatter with the rice growth (Clauss *et al.*, 2017)

*al.*, 1999; Shao *et al.*, 2001), ENVISAT/ASAR (Bouvet *et al.*, 2009), TerraSAR-X (Taylor *et al.*, 2011) and ALOS PALSAR (Ling *et al.*, 2010; Zhang *et al.*, 2009). However, these SAR data limit themselves in terms of the cost, their availability and temporal resolution (Tian *et al.*, 2018).

The advent of freely available Sentinel 1A C Band satellite data launched by European Space Agency (ESA) has resolved the above problem by providing high spatial resolution of 20m x 22m in range and azimuth direction (10m x 10m pixel spacing) and temporal (12 days revisit time) resolution SAR data having dual polarization viz. VV and VH to monitor the complex phenological growth stage of rice. The combination of large temporal series of imageries enable to analyze the interaction of SAR backscatter coefficient with the rice till full maturity stage.

The objective of this study is to analyze the variation of backscatter coefficient throughout the rice growth stage using temporal acquired data of Sentinel-1A and to classify the rice and non-rice areas using thresholding approach. Nguyen *et al.*, 2016 used the time series algorithm using beginning date, heading date and the length for the growing season to extract the phenological parameters for rice mapping. These parameters were start date of season (DoS) which represents the minimum backscatter, date of maximum backscatter (DoM) which indicates the maximum backscatter reaches till ripening stage of rice and length of season (LoS) is the difference between maximum and minimum backscatter. These were used to estimate the thresholds for segregating the rice, built up and water features.

## Materials and Methods

### Study site

The study area chosen for paddy demarcation for the period of 2018 was the Ludhiana district which is a central part of Punjab (Figure 2). It is the most advanced agricultural district and play an important role in contribution to Punjab's agricultural crop production. Earlier, it was also being a part of Intensive Agriculture District

Programme (IADP) and thus become the foremost district of the country. Geographically, the district covers an area of 3767 km<sup>2</sup> consisting of eleven subgroups such as Khanna, Ludhiana I, Ludhiana II, Samrala, Jagraon, Mangat, Doraha, Dehlon, Pakhowal, Machiwara, Sidhwan Bet and Sudhar, out of which 3 lakh ha area is utilized for sowing purpose. The irrigation is mostly done through tubewells. The area comprises Indo-Gangetic alluvium which is drained by Satluj and its tributaries which makes it fit for agricultural practices. The major crops cultivated throughout the year in the region are different varieties of paddy and maize. The climatic variability in the region are tropical steppe, hot and semi-arid. Variation in temperature ranges from 1.2 °C to 5.8 °C with annual rainfall of 680mm. Air carries lots of moisture from ocean in monsoon time which starts from June last week and last upto September. Thus cause the region suitable for kharif crops.

### Datasets

The rice cultivation in the Ludhiana takes place from June to November period of time of every year. For that, the study used 12 Sentinel-1A (S1A) temporal SAR imageries at C band (5.405 GHz, wavelength = 5.546cm, incidence angle 30.64° to 36.79°) of kharif season. These are acquired by Copernicus in Interferometric Wide Swath (IW) imaging mode having pixel spacing of 10m x 10m. The Sentinel-2 optical data and google earth imagery were used for extracting the rice field of the region. Shuttle Radar Topographic Mission (SRTM) Digital Elevation Model (DEM) 30m, topographical data was obtained from USGS for removing the topographic effects in SAR imageries. Table 1 showed the various datasets used for mapping.

### Sentinel-1A (S1A) data and processing

Preprocessing of S1A imageries was done in Sentinel Application platform (SNAP) open source software (version 6.0) developed by European Space Agency (ESA). The Level 1 GRDH (ground range detected and high resolution) product of S1A time series data were

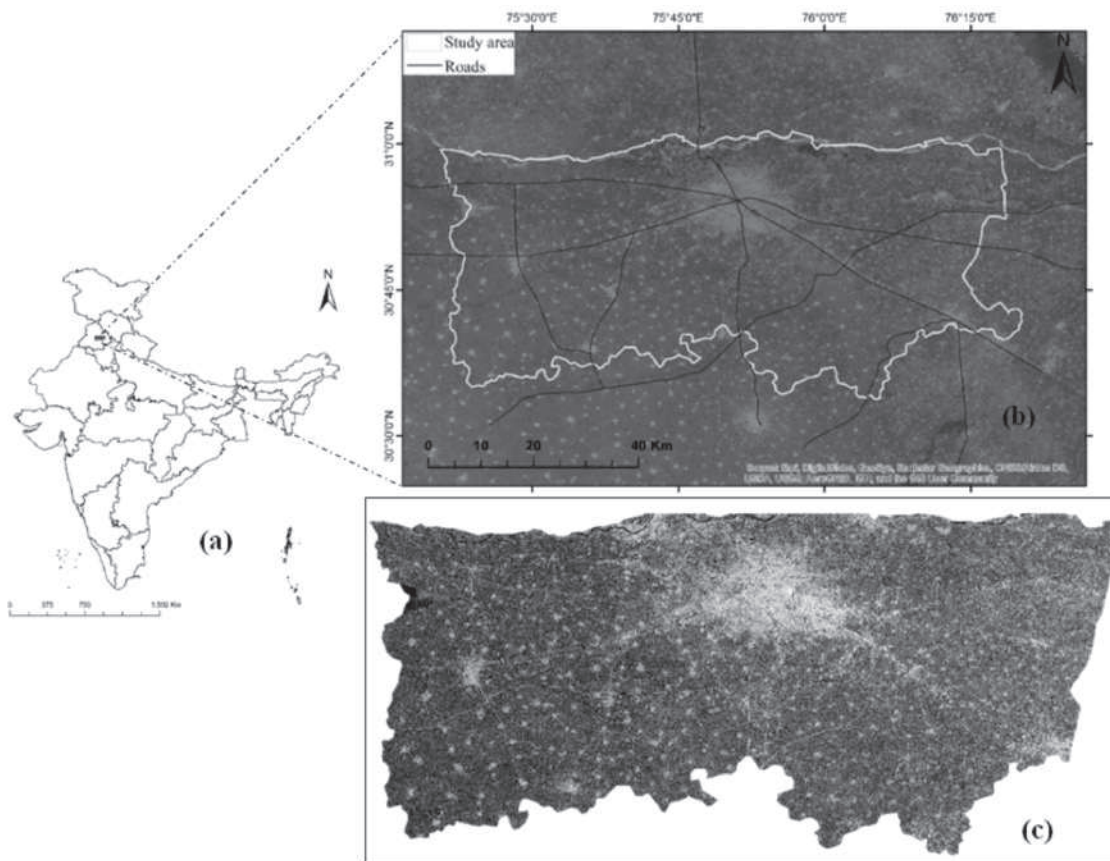


**Fig. 2.** Location of study site, Ludhiana, India (a) and (b). The band composite of SAR image (Red: Sigma0 VV Blue: Sigma0 VH Green: Sigma0 VV/Sigma0 VH) (c).

**Table 1.** List of datasets

Datasets	Resolution	Date of acquisition	Source
Sentinel-1A	20mx22m (range x azimuth)	13-Jun-18	<a href="https://scihub.copernicus.eu/dhus/">https://scihub.copernicus.eu/dhus/</a>
		25-Jun-18	
		7-Jul-18	
		19-Jul-18	
		31-Jul-18	
		12-Aug-18	
		24-Aug-18	
		5-Sep-18	
		29-Sep-18	
		11-Oct-18	
		23-Oct-18	
		16-Nov-18	
		Sentinel 2	
12-Jul-18			
26-Aug-18			
05-Oct-18			
25-Oct-18			
SRTM DEM	30m	09-Nov-18	<a href="https://earthexplorer.usgs.gov/">https://earthexplorer.usgs.gov/</a> Google Earth Pro
Google Earth imagery			

used with VH (vertical transmit, horizontal receive) polarization as it is proven to be more sensitive to monitor paddy rice growth than the VV (vertical transmit, vertical receive) polarization (Singha *et al.*, 2019) for rice mapping. The workflow for obtaining the backscattered coefficient ( $s^\circ$ ) included the five steps: (1) Radiometric calibration was performed to output as sigma naught ( $s^\circ$ ) bands, (2) Speckle filtering applied to remove the noise in the sigma naught bands, (3) SRTM 30m DEM was used for the correcting the topographic effect, (4) Area of region was masked out and backscatter values converted into decibel (DB) and (5) Finally, all the  $s^\circ$  bands were stacked separately for VH and VV polarization in DB unit.

### Optical and reference data

The Sentinel-2 optical imagery of corresponding growth stage of the rice and high resolution Google Earth imagery were used for digitizing the rice fields, built-up areas and water bodies. Total number of signatures manually

extracted were 96 rice, 73 built up and 62 water bodies.

### Temporal characteristics of backscattering coefficient with the different classes

Mean backscattered coefficient values of the preprocessed image time series was calculated for all the extracted classes by averaging the backscattered coefficient within the class polygon. These mean values were further used to analyze the temporal pattern of rice, built up and water class with the SAR backscattering during season period at VH and VV polarization. It was found that the backscatter coefficient values were high for built up areas and low for water bodies due to smooth surface reflection. For rice growing period, initially high backscatter values seen in time of land preparation followed by decreased in backscatter values during flooded rice fields, later the backscatter values gradually increased after rice transplantation and attained maximum value till ripening stage of rice (Figure 3, 4 and 5).

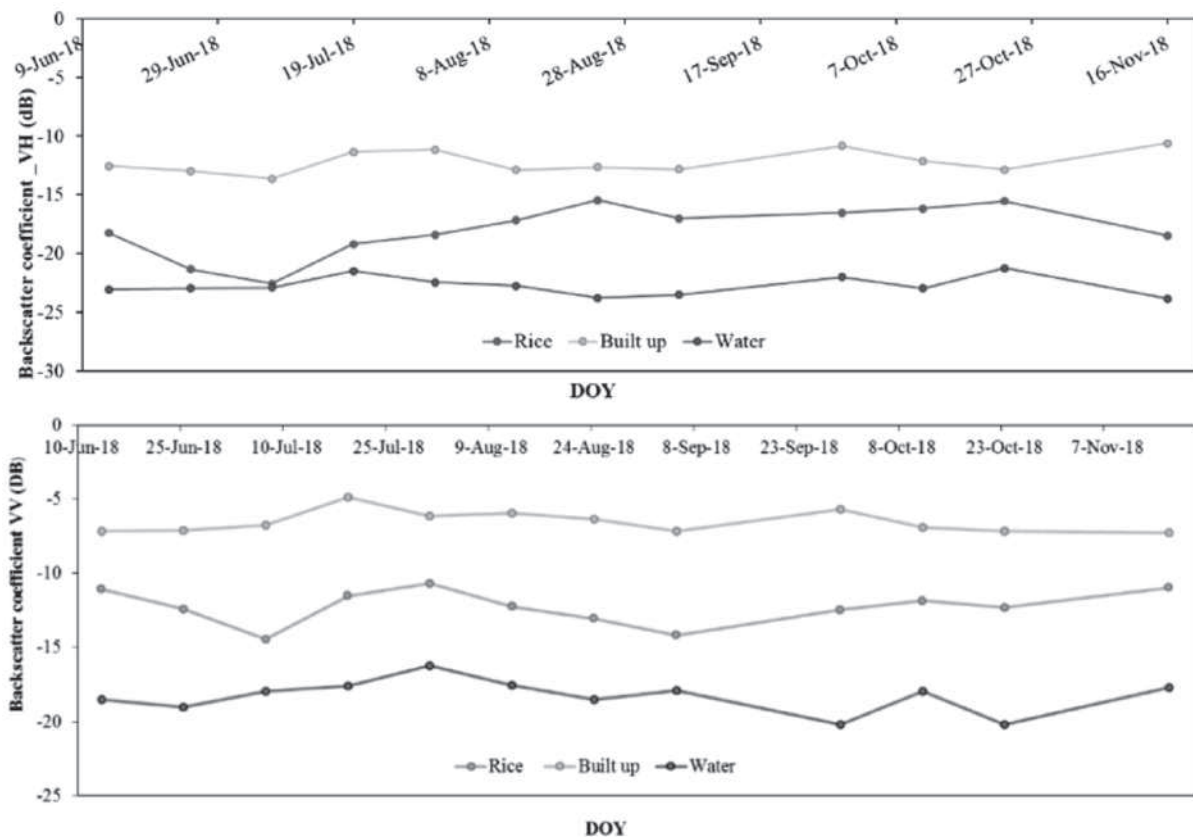
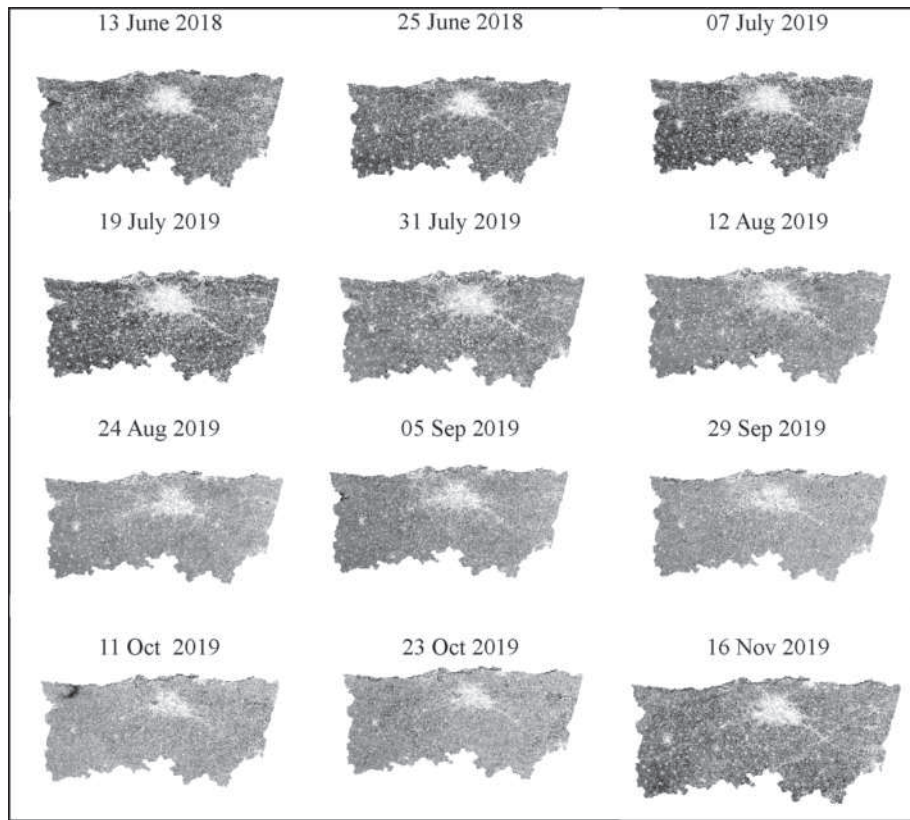
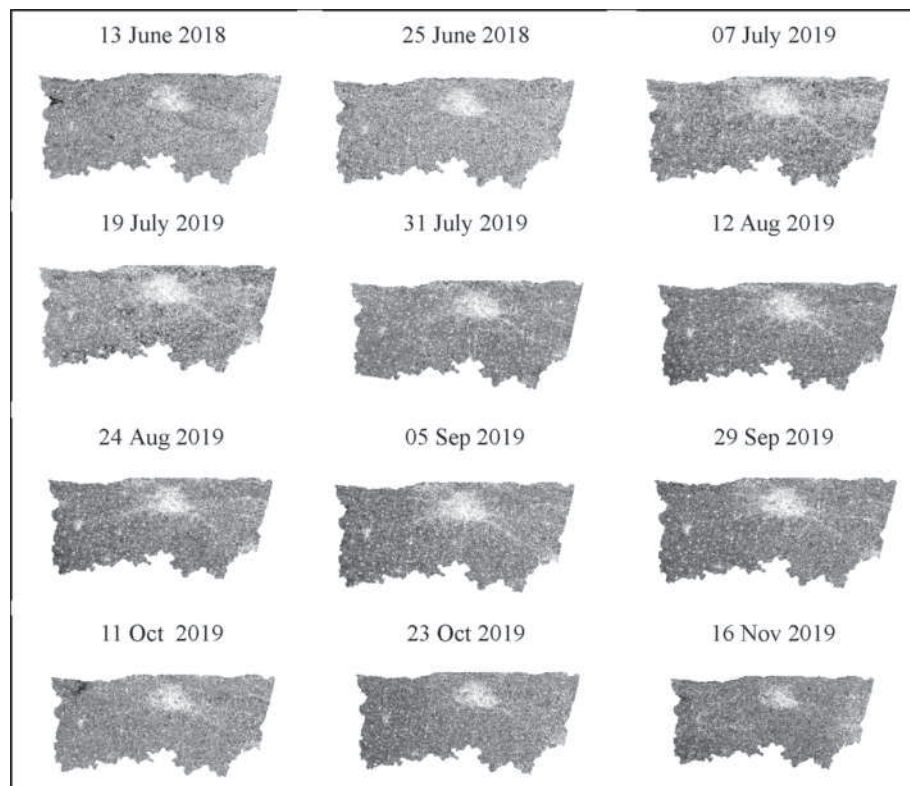


Fig. 3. Temporal behavior of SAR backscattering with rice, built up and water in VV and VH polarization



**Fig. 4.** Time series backscatter coefficient in VH polarization



**Fig. 5.** Time series backscatter coefficient in VV polarization

### Rice fields demarcation using threshold based classification approach

The thresholds based classification method was adopted in the study to demarcate the rice fields by calculating the thresholds for each class. It is based on time series algorithm used by Nguyen *et al.* (2016); Nguyen *et al.* (2015) who incorporated the beginning date, heading date and the length for the growing season to extract the phenological parameters for mapping rice. These phenological parameters were date of the start of season (DoS) that marked the backscatter changes from zero or negative to positive or the minimum backscatter that extends the period from season of start to first tiller appear, date of maximum backscatter (DoM) that indicates the backscatter reaches its maximum and stretch period from tillering till ripening stage of rice season and the length for the growing season (LoS) defined the range of maximum and minimum backscatter that is the difference between DoS and DoM.

To discriminate the rice fields from other land use and land cover class such as built up and water bodies, thresholds were determined from

the time series backscatter coefficient of cross polarization VH. The indicator such as minimum and maximum backscatter were used to calculate the thresholds for segregating the non-rice areas viz. manmade and water features (Phan *et al.*, 2018). The range indicator that gives the maximum increment change occurred in backscatter values which also represents the shortest rice growth cycle. Thus, it is used to derive threshold for the rice field. In this study, threshold  $a=5.0$  (dB) was applied to map rice areas, threshold  $b$  and  $c$  were chosen as  $-19$  (dB) and  $-20$  (dB) (Eq.1). Figure 6 showed the sequential steps followed for delineating the rice and non-rice areas.

$$\begin{aligned} \text{Range } \sigma^{\circ} \text{ VH} \geq a \text{ (dB), then rice fields} \\ \text{Min } \sigma^{\circ} \text{ VH} \geq b \text{ (dB), then built up areas} \\ \text{Max } \sigma^{\circ} \text{ VH} \leq c \text{ (dB), then water} \end{aligned} \quad \text{Eq. (1)}$$

### Results and Discussions

The phenological parameters such as minimum, maximum backscatter and range of backscatter are shown in Figure 6(a), (b) & (c). Mostly the areas of rice cultivation (DoS) of

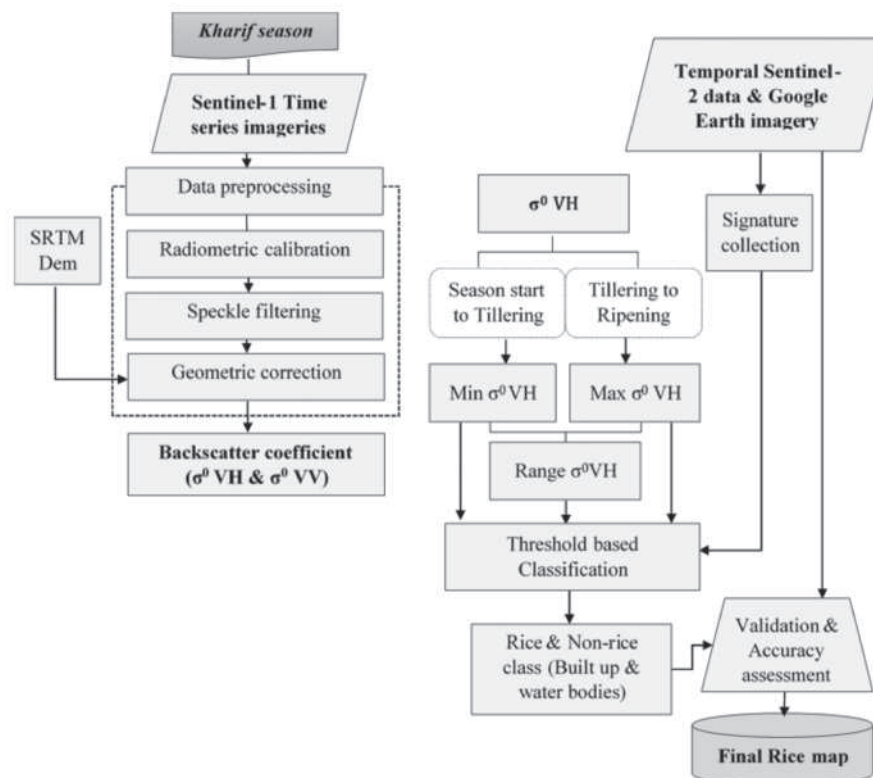


Fig. 6. Methodology for rice area mapping

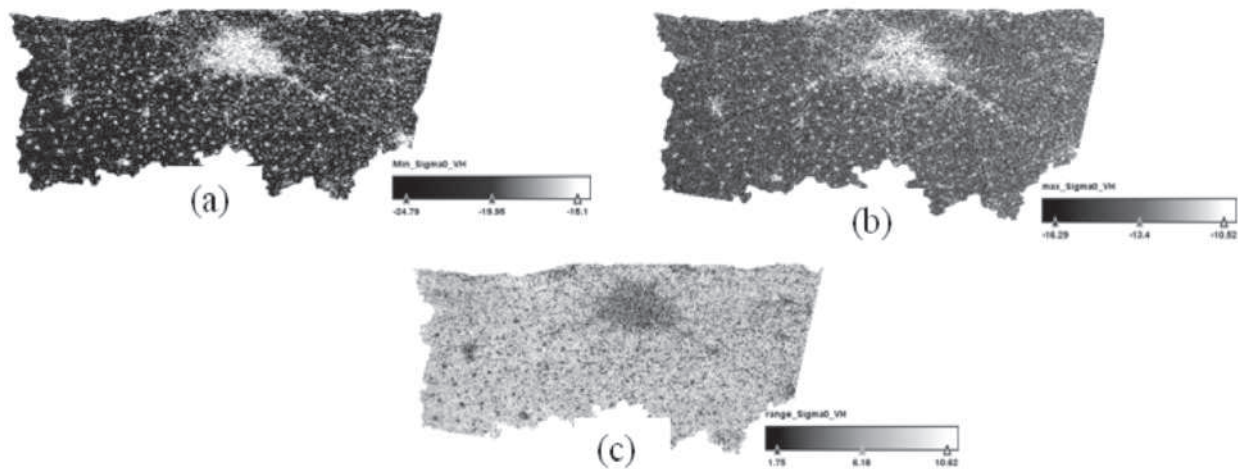


Fig. 7. Minimum backscatter, maximum backscatter and range of backscatter

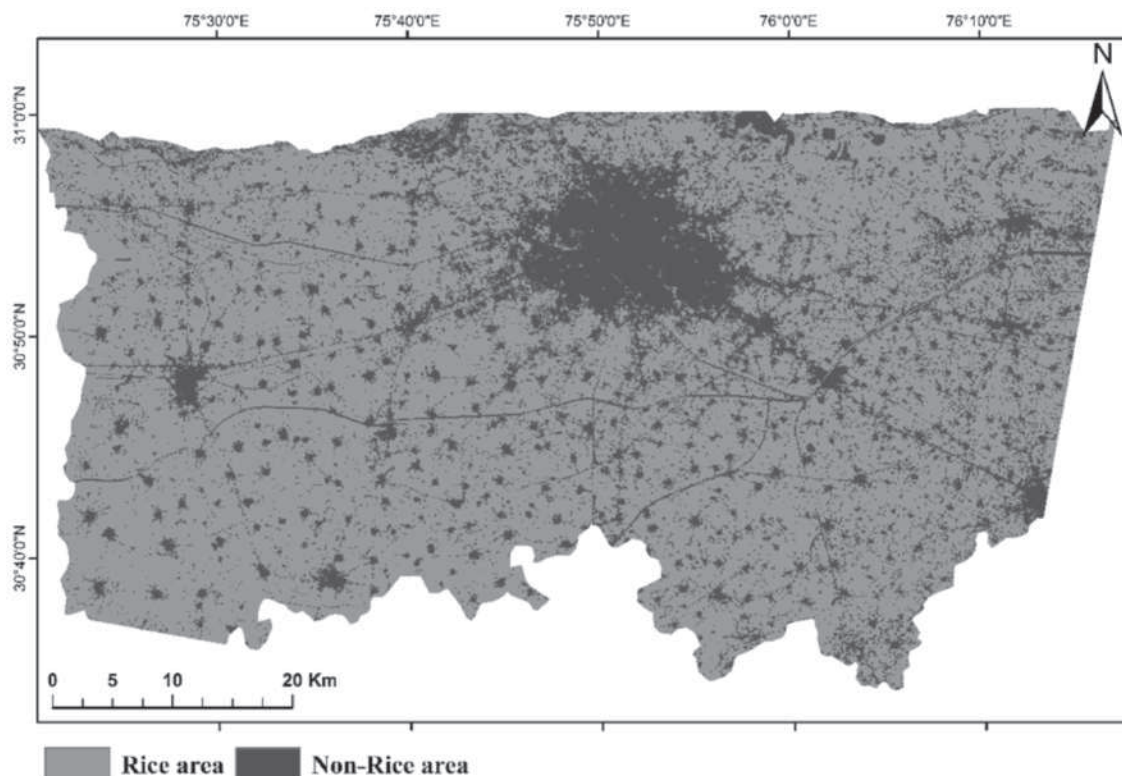


Fig. 8. Estimated rice cropland from Sentinel 1 time series of Ludhiana for kharif season 2018

Ludhiana are seen in the beginning of monsoon season in northern parts of India around June 2018 to mid of July 2018. The DoM ranges from July end to beginning of November 2018.

The mapped rice fields were produced for the kharif season of 2018 by applying the threshold of 5 dB for the Ludhiana district is shown in Figure 8. The total area of rice estimated from

satellite is 2.54 lac ha whereas the ground collected surveyed by Punjab Agricultural University (PAU) showed 2.57 lac ha rice area for 2018. Hence it showed good agreement. However, it was seen that some area of Ludhiana district such as Machiwara, Samrala and Khanana with approximately 17000 ha area was not available during rice mapping through SAR data

**Table 2.** Confusion matrix

		Classified image			User accuracy (%)
		Rice	Non Rice	Total	
Reference collected points	Rice	96	0	96	100
	Non Rice	17	118	135	12.59
	Total	113	118	231	
	Producer accuracy (%)	84.95	100		

The accuracy assessment has been performed to evaluate the accuracy of classification using signatures collected from reference data of 2018 *kharif* season as shown by the confusion matrix (Table 2). The overall accuracy of the classification is 92.64% with kappa coefficient is 0.85. It was observed that some of the pixels of water in the canal got mixed with the rice class in eastern part, otherwise pixels were classified well as rice in other parts of the image.

## Conclusion

The goal of this study was to demonstrate the use of SAR data for rice mapping of the Ludhiana region of *kharif* season 2018. For this purpose, Sentinel-1A time series imageries has been used throughout the growing season of rice. From the temporal characteristics of rice with the radar backscatter it was found that the VH polarization was more sensitive to rice growth than the VV polarization.

Threshold based classification method was exploited to map the rice fields with overall classification accuracy achieved as 92.64% and kappa coefficient is 0.85. The mapped rice area was estimated as 2.54 lac ha which showed good agreement with the ground statistics collected by PAU as 2.57 lac ha. Therefore, Sentinel-1A temporal data has proven to be competent tool in monitoring the rice growth at a regional scale.

## References

Bouvet, A., Toan, T. Le and Lam-dao, N. 2009. Monitoring of the Rice Cropping System in the Mekong Delta Using ENVISAT / ASAR Dual Polarization Data. *IEEE Transactions on Geoscience and Remote Sensing*, **47**(2): 517-526.

Clauss, K., Ottinger, M. and Kuenzer, C. 2017. Mapping rice areas with Sentinel-1 time series

and superpixel segmentation. *International Journal of Remote Sensing*, **39**(5): 1399-1420. <https://doi.org/10.1080/01431161.2017.1404162>

Dong, J. and Xiao, X. 2016. Evolution of regional to global paddy rice mapping methods/ : A review. *ISPRS Journal of Photogrammetry and Remote Sensing*, **119**: 214-227. <https://doi.org/10.1016/j.isprsjprs.2016.05.010>

FAOSTAT: FAO Statistical Databases (Food and Agriculture Organisations of the United Nations) Databases – UW-Madison Libraries, <http://digital.library.wisc.edu/1711.web/faostat> accessed on October 2018.

Genc, L., Inalpulat, M., Kizil, U. and Aksu, S. 2014. Determination of Paddy Rice Field Using Landsat 8 Images. In *International Conference on Biological, Civil and Environmental Engineering (BCEE-2014)* (pp. 182-185). Dubai.

Hoang, H. K., Bernier, M., Member, S., Duchesne, S., and Tran, Y.M. 2016. Rice Mapping Using RADARSAT-2 Dual- and Quad-Pol Data in a Complex Land-Use Watershed/ : Cau River Basin ( Vietnam ). *IEEE Journal of Selected Topics in Applied Earth Observations and Remote Sensing*, **9**(7): 3082-3096.

Holecz, F., Monaco, S., Dwyer, E., Schmid, B., Frei, U. and Fischer, R. 2000. An Operational Rice Field Mapping Tool Using Spaceborne Sar Data. In *Ers-envisat Symposium*. Göteborg.

Ishitsuka, N. 2018. Identification of Paddy Rice Areas Using SAR/ : Some Case Studies in Japan, **52**(March 2017), 197-204.

Kurosu, T., Fujita, M. and Chiba, K. 1995. Monitoring of rice crop growth from space using the ERS-1 C-band SAR. *IEEE Transactions on Geoscience and Remote Sensing*, **33**(4): 1092-1096.

Ling, F., Li, Z., Chen, E., Tian, X., Bai, L. and Wang, F. 2010. Rice areas mapping using Alos Palsar FBD data considering the bragg scattering in L-

- band Sar Images of rice fields. In *IEEE International Geoscience and Remote Sensing Symposium* (pp. 1461–1464).
- Mccloy, K.R., Smith, F.R. and Robinson, M.R. 1987. Monitoring rice areas using LANDSAT MSS data. *International Journal of Remote Sensing*, **8**(5): 741-749. <https://doi.org/10.1080/01431168708948685>
- Nguyen, D.B., Gruber, A. and Wagner, W. 2016. Mapping rice extent and cropping scheme in the Mekong Delta using Sentinel-1A data. *Remote Sensing Letters*, **7**(12): 1209-1218. <https://doi.org/10.1080/2150704X.2016.1225172>
- Nguyen, D., Wagner, W., Naeimi, V. and Cao, S. 2015. Rice-planted area extraction by time series analysis of ENVISAT ASAR WS data using a phenology-based classification approach: A case study for Red River Delta, Vietnam. *International Archives of the Photogrammetry, Remote Sensing and Spatial Information Sciences - ISPRS Archives*, **40**(7W3), 77–83. <https://doi.org/10.5194/isprsarchives-XL-7-W3-77-2015>
- Okamoto, K. and Fukuhara, M. 1996. Estimation of paddy field area using the area ratio of categories in each mixel of Landsat TM. *International Journal of Remote Sensing*, **17**(9): 1735-1749. <https://doi.org/10.1080/01431169608948736>
- Park, S., Im, J., Park, S., Yoo, C., Han, H. and Rhee, J. 2018. Classification and mapping of paddy rice by combining landsat and SAR time series data. *Remote Sensing*, **10**(3): 447. <https://doi.org/10.3390/rs10030447>
- Phan, H., Le Toan, T., Bouvet, A., Nguyen, L.D., Duy, T.P. and Zribi, M. 2018. Mapping of rice varieties and sowing date using X-band SAR data. *Sensors* **18**(1): 316. <https://doi.org/10.3390/s18010316>
- Ribbles, F. and Toan, T.LE. 1999. Rice field mapping and monitoring with RADARSAT data. *International Journal of Remote Sensing*, **20**(4): 745-765. <https://doi.org/10.1080/014311699213172>
- Shao, Y., Fan, X., Liu, H., Xiao, J., Ross, S., Brisco, B., ... Staples, G. 2001. Rice monitoring and production estimation using multitemporal RADARSAT. *Remote Sensing of Environment*, **76**: 310-325.
- Singha, M., Dong, J., Zhang, G. and Xiao, X. 2019. High resolution paddy rice maps in cloud-prone Bangladesh and Northeast India using Sentinel-1 data. *Scientific Data*, **6**(1): 26. <https://doi.org/10.1038/s41597-019-0036-3>
- Stroppiana, D., Boschetti, M., Azar, R., Barbieri, M., Collivignarelli, F., Gatti, L., ... Holecz, F. 2019. In-season early mapping of rice area and flooding dynamics from optical and SAR satellite data. *European Journal of Remote Sensing*, **52**(1): 206-220. <https://doi.org/10.1080/22797254.2019.1581583>
- Taylor, P., Pei, Z., Zhang, S., Guo, L., Mcnairn, H., Shang, J., ... Jiao, X. 2011. Rice identification and change detection using TerraSAR-X data. *Canada Journal of Remote Sensing*, **37**(1): 151-156. <https://doi.org/10.5589/m11-025>
- Teluguntla, P., Ryu, D., George, B., Walker, J.P. and Malano, H.M. 2015. Mapping flooded rice paddies using time series of MODIS imagery in the Krishna River Basin, India. *Remote Sensing*, **7**, 8858-8882. <https://doi.org/10.3390/rs70708858>
- Tian, H., Wu, M., Li, W. and Niu, Z. 2018. Mapping early, middle and late rice extent using sentinel-1A and Landsat-8 data in the Poyang Lake Plain, China. *Sensors*, **18**(1): 185. <https://doi.org/10.3390/s18010185>
- Toan, T. Le, Ribbles, F., Wang, L.-F., Floury, N., Ding, K.-H., Kong, J. A., ... Kurosu, T. 1997. Rice crop mapping and monitoring using ERS-1 data based on experiment and modeling results. *IEEE Transactions on Geoscience and Remote Sensing*, **35**(1): 41-56.
- Turner, M.D. and Congalton, R.G. 1998. Classification of multi- temporal SPOT-XS satellite data for mapping rice fields on a West African floodplain. *International Journal of Remote Sensing*, **19**(1): 21–41. <https://doi.org/10.1080/014311698216404>
- Zhang, M., Lin, H., Wang, G., Sun, H. and Fu, J. 2018. Mapping paddy rice using a convolutional neural network ( CNN ) with Landsat 8 datasets in the. *Remote Sensing*, **10**(11): 1840. <https://doi.org/10.3390/rs10111840>
- Zhang, Y., Wang, C., Wu, J. and Qi, J. 2009. Mapping paddy rice with multitemporal ALOS / PALSAR imagery in southeast China. *International Journal of Remote Sensing*, **30**(23): 6301-6315. <https://doi.org/10.1080/01431160902842391>